6 Model of Tin Ore Formation

6.1 Origin of Tin Granites

The origin of tin granites is part of the ongoing discussion on the origin of granitic rocks in general. There is an historic polarization in petrogenetic models for granites which are seen either in idealized terms of intracrustal melting or of differentiation of mantle melts. More recent chemical and isotopic data suggest a multiple-source and open-system model for the formation of granitic rocks, in which continental silicic magmatism is seen as a result of variable physical and chemical interaction of upper mantle and continental crust, i.e. crust-mantle mixtures rather than either pure differentiates of mantle magmas or pure products of crustal anatexis (Hildreth 1981; Holden et al. 1987; Marsh 1987; DePaolo 1988). The state of crustal stress will critically control the process time for chemical interaction between ponded melts and their host rocks in a lower crustal environment, and together with crustal thickness (length of percolation column) will also define the process time for the internal evolution of silicic melts during their rise to upper crustal levels (Pitcher 1987; Hildreth and Moorbath 1988; Lipman 1988). Crustal melting and mixing of crustal and subcrustal melt portions play its largest role in the high-temperature deeper (lower crustal) levels of magmatic systems. At shallower levels, assimilation is minor and crystal fractionation appears to be the dominant process controlling the magmatic evolution of high-silica melts (Farmer and DePaolo 1983, 1984; Musselwhite et al. 1989).

The fundamentally continuous nature of granite petrogenesis has been demonstrated with the help of Sr and Nd isotope data for the Mesozoic and Tertiary granitic rocks of the southwestern USA (Farmer and DePaolo 1983, 1984), for the Paleozoic batholiths of southeastern Australia (McCulloch and Chappell 1982), and for the Paleozoic to Cenozoic granite belts along the western margin of South America (Pankhurst et al. 1988). These granite provinces cover in terms of the petrogenetic parameters of initial ϵ_{Sr}-ϵ_{Nd} a broad concave compositional field, defined by a negative correlation trend for values of ϵ_{Sr} up to 100, and relatively constant ϵ_{Nd} values for a wide range of ϵ_{Sr} of >100.

Figure 80 is a compilation of the available initial Sr and Nd data on tin granites. The data cover a wide compositional range similar to the variation in other tin-
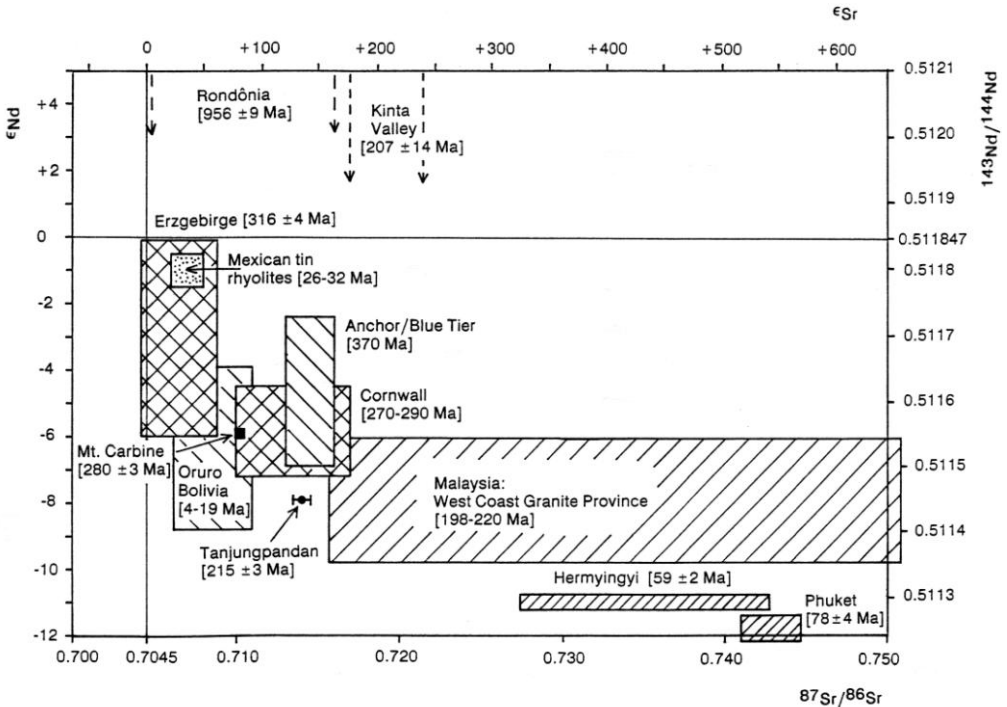
Fig. 80. Initial Sr and Nd isotope data for granitic rocks from several tin provinces. Data sources: Phuket (Cobbing written commun. 1989; Putthapiban et al. 1986); Hermyingyi, Burma (Cobbing written commun. 1989; Darbyshire and Swainbank 1988); Tanjungpandan, Indonesia (Darbyshire 1988b; Darbyshire pers. commun. 1988); East and West Coast granites, Malaysia (Liew and McCulloch 1985); Mt. Carbine, North Queensland, and Anchor Mine, Tasmania, Australia (Higgins and Sun 1988); Cornwall (Darbyshire and Shepherd 1988); Oruro, Bolivia (Redwood 1986); Erzgebirge, Germany (Gerstenberger 1989); Sierra Madre Occidental, Mexico (Ruiz 1988); Cordillera Real (McNutt and Clark 1983; Miller and Harris 1989); Kinta Valley, Malaysia (Schwartz and Askury 1989); Rondônia, Brazil (Priem et al. 1989).

barren granite provinces (cf. DePaolo 1988), and do not suggest any specific origin for tin granites which would set them apart from non-tin granites. The discussion of these data must take into account that highly fractionated melts have low Sr and high Nd concentrations and are thus susceptible, even with small amounts of assimilation, to large shifts in $^{87}Sr/^{86}Sr$ but not in $^{143}Nd/^{144}Nd$. The same limitation applies also to Pb isotope systematics of contaminated mantle melts which are readily equilibrated with external Pb by minor crustal input. The Sr system in late, highly fractionated melt phases

may also shift towards higher Sr initials as a consequence of the internal Rb-Sr evolution in large melt reservoirs (McCarthy and Cawthorn 1980). On the other hand, the postmagmatic rubidium metasomatism important in some tin granites can result in too low apparent Sr initial ratios (Gerstenberger 1989). The importance of mantle-derived components in granitic rocks can be adequately assessed only by Nd isotope data.

The source material of the Malaysian Main Range granites of the SE Asian tin belt with $\epsilon_{Nd}(T)$ of -6 to -10 must be predominantly Phanerozoic crust with a Nd model age of 1300-1700 Ma (Liew and McCulloch 1985). Involvement of mantle material would require mixing with still older crustal rocks, which is, however, not likely in view of the upper intersection ages of U-Pb zircon reverse discordia of 1500-1700 Ma (Liew and Page 1985). The eastern granite province in SE Asia (East Coast granite population), on the other hand, has a large spread in $\epsilon_{Nd}(T)$ values of -0.7 to -6.2 and appears to have variable input of mantle material (Liew and McCulloch 1985; Darbyshire pers. commun. 1988). The western granite province of the SE Asian tin belt (samples from Phuket and Hermyingyi) has $\epsilon_{Nd}(T)$ values of -11 to -12, which suggests a dominantly crustal source at least 1800 Ma old (Darbyshire unpubl. data).

The Nd and Sr isotope data from tin granites in Bolivia (Cordillera Real), Tasmania (Blue Tier batholith), North Queensland (Mt. Carbine) and of the Erzgebirge, as well as from tin porphyries in Bolivia and Mexico, suggest a variable degree of involvement of mantle material. This is particularly likely for the Erzgebirge tin granites which have $\epsilon_{Nd}(T)$ values of 0.0 to -6.0 (Gerstenberger 1989), and for the Mexican tin rhyolites with $\epsilon_{Nd}(T)$ around -1 (Ruiz 1988).

The data in Fig. 80 do not allow assigning an exclusively crustal origin to all tin granites, although crustal material is probably the dominant source of tin granites. This is true, however, for most tin-barren granites as well. Continental setting is a worldwide feature of tin-tungsten deposits and their associated igneous rocks. The tectogenetic environments of tin granites and porphyries are:
1. Postorogenic magmatism in continental collision belts, i.e. Permo-Triassic tin belt in SE Asia (Mitchell 1977; Beckinsale 1979), Hercynian tin provinces in western and central Europe (Mitchell 1974; Holder and Leveridge 1986).
2. Internal zones of active continental margins (back-arc regions), i.e. Tertiary tin porphyries in Bolivia, Mexico, eastern Siberia, USSR (Sillitoe 1976), Cretaceous-Tertiary tin granites in Thailand and Burma (Beckinsale 1979).
3. Intracontinental rift zones, i.e. Triassic tin granites in northern Bolivia (Kontak et al. 1984), Cretaceous tin granites in southern China (Chen

Guoda 1989), Cretaceous tin granites in Nigeria (Bowden and Kinnaird 1984), Precambrian tin granites in Rond"nia, Brazil (Sillitoe 1974), Precambrian Bushveld granites (Hunter 1973).

The tectonic setting of tin deposits may reflect a critical physical parameter for tin formation, i.e. a thick crust which permits process space and time for a high degree of partial melting and extended fractional crystallization. More than 25 % partial melt during crustal anatexis is probably a precondition for large-scale magma segregation. A smaller amount of silicic melt is likely to remain trapped in-situ as migmatite (Thompson and Connolly 1990). Magma segregation and intrusion into an upper crustal level is favoured by brittle lithosphere in crustal extensional zones.

6.2 Time-Space Framework

The spatial association of tin ore deposits with granitic rocks is documented by a very large observational basis and is generally accepted. However, all genetically more specific interpretations meet less unanimous consent. The postmagmatic-epigenetic nature of hydrothermal tin deposits is a consequence of their geometry and age relative to the host granite. Radiometric age data commonly give a temporal hiatus between solidification of the granitic country rock and hydrothermal ore formation which can be on the order of several million years. The Cornwall situation is summed up in the Rb-Sr isochron data of Darbyshire and Shepherd (1985) in Table 8.

Table 8. Rb-Sr isochron data for granitic rocks and hydrothermal fluids from tin deposits (fluid inclusions in vein quartz) in Cornwall. Data from Darbyshire and Sheppard (1985)

Locality	Age	$^{87}Sr/^{86}Sr_i$	
Carnmenellis pluton	290 ± 2 Ma	0.713	± 4
Bodmin Moor pluton	287 ± 2 Ma	0.717	± 2
St. Austell pluton	285 ± 4 Ma	0.7095	± 9
Dartmoor pluton	280 ± 1 Ma	0.7094	± 3
Meldon Elvan (aplite)	279 ± 2 Ma	0.710	± 2
Wherry Elvan (aplite)	282 ± 6 Ma	0.712	± 3
Brannel Elvan (aplite)	270 ± 9 Ma	0.715	± 3
South Crofty mine (quartz)	269 ± 4 Ma	0.7147	± 3
Geevor mine (quartz)	270 ± 15 Ma	0.712	± 1
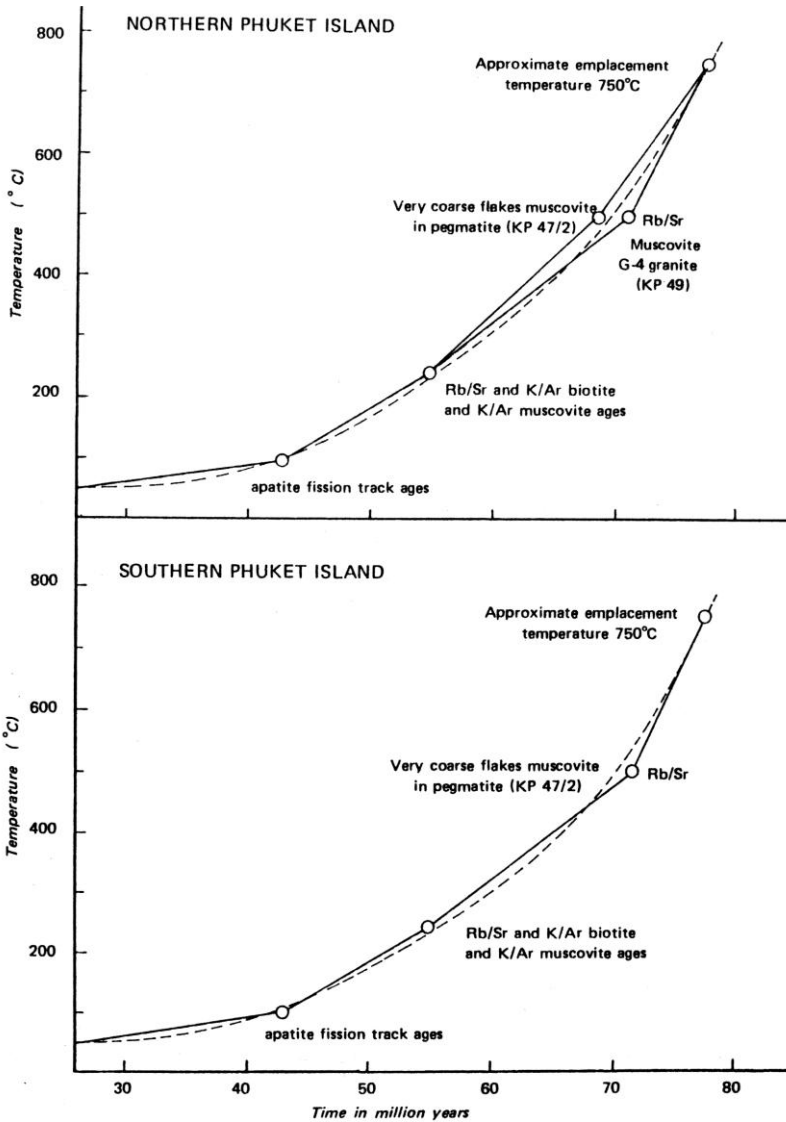
Fig. 81. Cooling history of the Phuket tin granites (Putthapiban et al. 1986:62). Emplacement age of granites: 78 ± 4 Ma (Rb-Sr isochron with inital $^{87}Sr/^{86}Sr$ 0.7428 ± 18)

K-Ar data suggest continued hydrothermal activity associated with the Cornwall granites into the Mesozoic (Halliday 1980; Jackson et al. 1982; Stone and Exley 1986). Long-lived fluid circulation induced by radiogenic heat production in highly fractionated granitic rocks with >8-10 ppm U ("high heat production granites"; Fehn et al. 1978; Darnley 1986) is generally believed to

be responsible for intermediate- and low-temperature processes with a large spectrum of metal concentrations (F, Ba, U, Pb, Zn, Ag, Au, Sb, Co, Bi) of epithermal formation (50-300°C). The internal radiogenic energy released in "high heat production granites" seems, however, to be insufficient for any substantial redistribution of tin, as noted by Fehn (1985) for the Cornwall province.
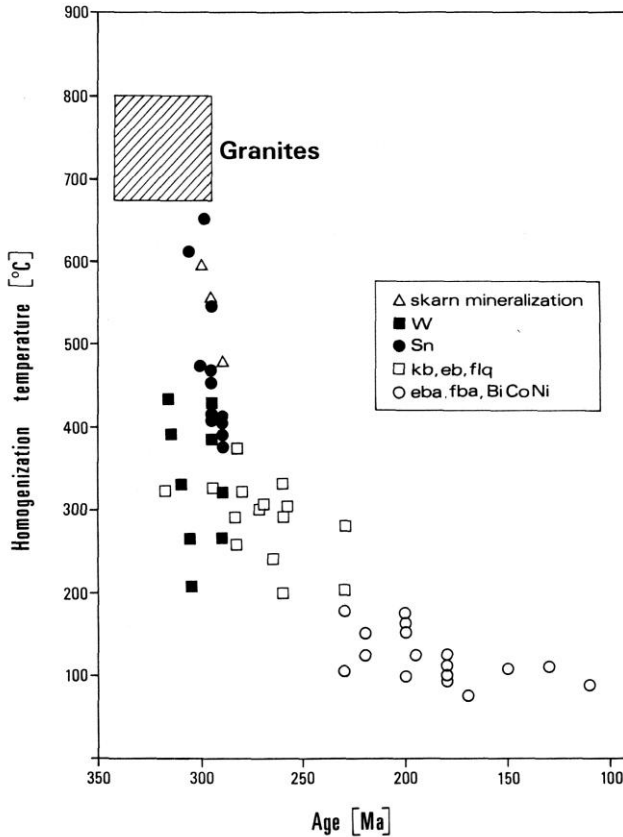
Fig. 82. Cooling history of the Erzgebirge granites according to radiometric and fluid-inclusion data from hydrothermal mineral assemblages of the early Sn-W mineralization and subsequent epithermal F-Ba-Ag-Pb-Zn-Bi-Co-Ni-U mineralization stages. (Thomas and Tischendorf 1987:31)

A similarly extended thermal (and hydrothermal) history has been documented for the Phuket granites in southern Thailand by a combination of Rb-Sr, K-Ar and fission track ages (Fig. 81) (Putthapiban et al. 1986). In the

Erzgebirge tin province, numerous U-Pb, Rb-Sr and K-Ar age data together with homogenization temperatures of fluid inclusions define a hydrothermal cycle lasting over 150 Ma (Fig. 82) (Thomas and Leeder 1986; Thomas and Tischendorf 1987).

The temperature-time diagrams demonstrate that tin granite provinces are characterized by persistent heat anomalies and have therefore long-lasting hydrothermal activity. The time period of tin mineralization can be of the order of several million years as shown by high-resolution $^{40}Ar/^{39}Ar$ age data from the Panasqueira Mine, Portugal, which give a duration of cassiterite deposition of greater than 4 million years (Fig. 83) (Snee et al. 1988). The multiphase nature and extended life span of both granite magmatism and tin mineralization require a composite magmatic system, large-scale fluid circulation and a long-lived fluid reservoir.
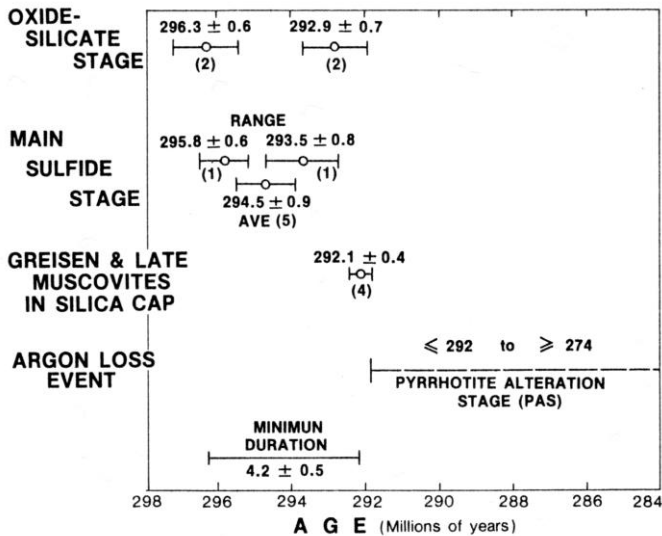
Fig. 83. Detailed $^{40}Ar/^{39}Ar$ geochronology of the Panasqueira tin-tungsten deposit, Portugal (Snee et al. 1988:349). Substantial tin mineralization is associated with the "oxide-silicate stage" (quartz-muscovite-tourmaline-arsenopyrite-cassiterite-wolframite) and the "main sulfide stage"

The generally postmagmatic character of tin mineralization (relative to the immediate granite wall rocks) led Stemprok (1967) to the concept of a para-genetic relationship between tin ore and granitic rocks, which sees the origin of tin-bearing solutions in deep crustal or subcrustal regions. The association of tin deposits and granitic rocks, particularly the frequent localization of tin ore in granite contact zones, was interpreted not as a phenomenon of

chemical consanguinity but as a physical consequence of joint lineament-controlled permeability conditions for both granitic melts and hydrothermal solutions. However, this concept of extremely large-scale fluid circulation provides no explanation for the chemical specialization of the ore fluids and of tin granites. In addition, the great increase in solubility of water in granitic melts with increasing pressure probably excludes the coexistence of a melt plus an aqueous fluid phase even at intermediate crustal levels.

6.3 The Magmatic System

A high degree of fractionation is the general feature of granitic rocks associated with tin mineralization. The importance of fractional crystallization is shown by the systematic distribution patterns of major and trace elements. Major elements trend towards the thermal minimum of the Qz-Ab-Or-H_2O system at low pressure, i.e. equilibration to the shallow intrusion environment. Depletion trends of Ca, Mg, Fe, Ti, and complementary depletion and enrichment trends of compatible and incompatible trace elements together with the trend of increasing negative Eu anomaly all indicate fractional crystallization. These chemical evolution trends correlate with temporal and spatial distribution patterns, with the more strongly fractionated melt portions becoming increasingly younger and smaller in volume. Explanations of these phenomena by hypotheses invoking a variable rate of partial melting in the roots of the magmatic system, or by variable melt-restite mixing ratios are inadequate since the linear log-log trace element correlation trends in tin granite suites leave little room for assimilation/contamination as a petrogenetically dominant process. Such processes may play an important role in the deep crust (DePaolo 1981), i.e. in the magmatic evolution at a stage prior to the geochemically documented fractional crystallization sequence.

The synoptic diagrams of Fig. 84 summarize the behaviour of tin in the granite suites discussed earlier. The linear correlation of whole-rock tin content and the two indicators of differentiation, Rb/Sr and TiO_2 in log-log plots is in accordance with the model of a dominant role of fractional crystallization

---

Fig. 84 (next page). The correlation lines of the granitic sample suites discussed above in the reference system log[TiO_2]-log[Sn] and log[Rb/Sr]-log[Sn], respectively. Data on Hercynian tin granites of Portugal from Lehmann (1987). Solid lines are statistically significant at a level of certainty of >99.9 %. Global reference fields from Taylor and McLennan (1985) and Rösler and Lange (1976)
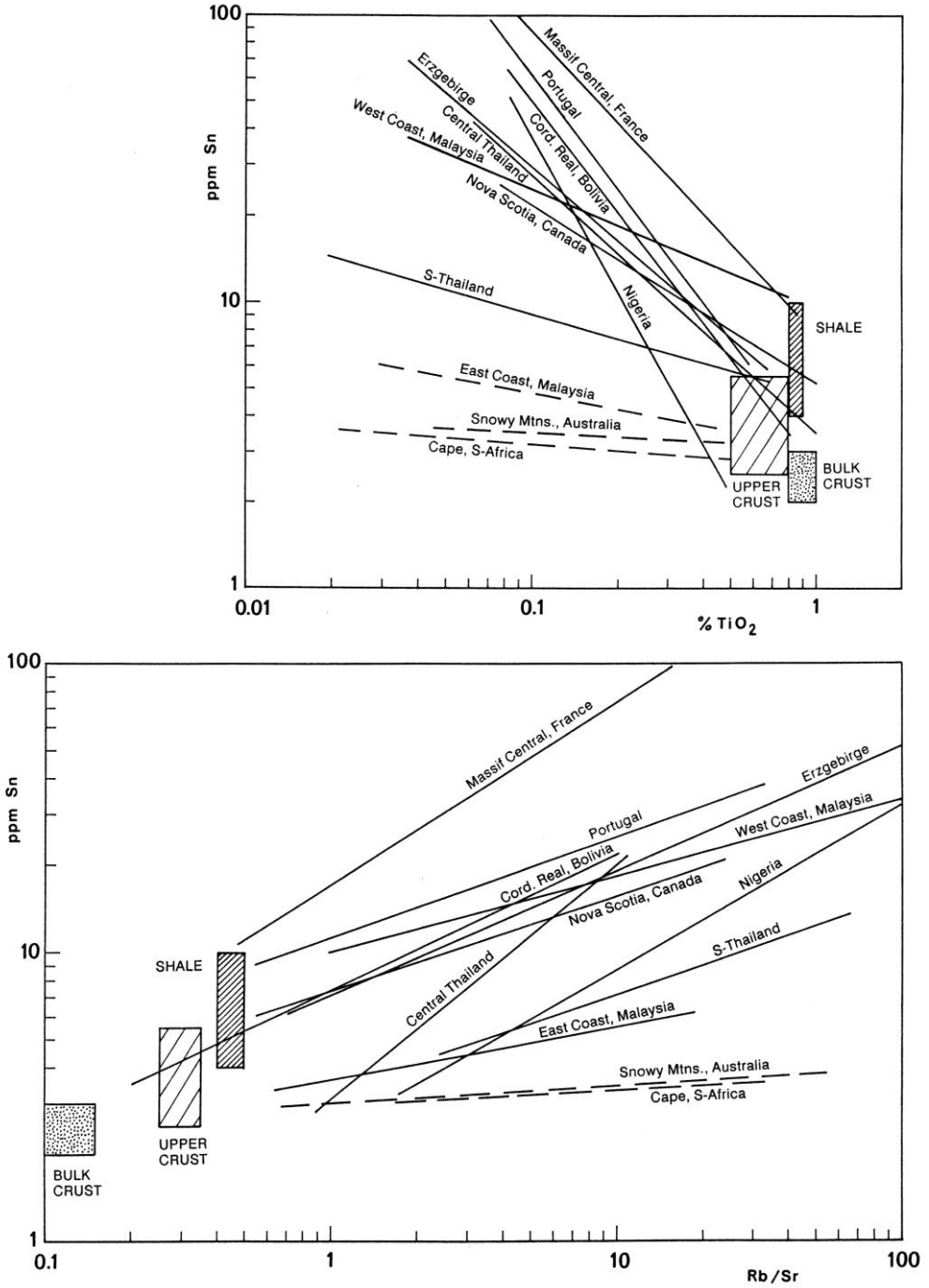
Fig. 84. For legend see previous page

during the magmatic evolution of these rocks (mixing processes result in hyperbolic correlation patterns in log-log space). All fractionation suites can be traced back to Sn levels of ≤10 ppm in their least-evolved portions, most even down to 5 ppm Sn. The assumption that the source material of tin granite suites may already be enriched in tin beyond average crustal levels is therefore not justified. With partial melting rates in anatectic granodiorite-granite systems in the range of 20-50 % (Compston and Chappell 1979) and moderately incompatible behaviour of tin ($\overline{D}_{Sn}$restite/melt = 0.5) bulk-crust material can be expected to yield partial melts with at least 5 ppm Sn.

The comparison with the global reference field for shales suggests correspondingly higher Sn contents in partial melts derived from argillaceous material. The relatively large range of tin contents in shales is, however, in part a consequence of analytical problems with older data derived by optical emission spectrography which tend to be too high (Turekian and Wedepohl 1961; Vinogradov 1962 in Rösler and Lange 1976). Analytical data from neutron activation spectrometry (Hamaguchi et al. 1964), atomic absorption spectrometry (Terashima and Ishihara 1982) and X-ray fluorescence spectrometry (Lehmann et al. 1988) consistently give a shale mean of 3-5 ppm Sn. Partial melting of such material, given an incompatible behaviour of tin, can therefore yield a granitic melt with 5-10 ppm Sn. Pelitic source material is probable for the S-type Hercynian granite suites of western Europe and the Triassic Main-Range granite belt of the SE Asian tin province, which may explain the relatively high tin contents of 5-10 ppm in the least-evolved portions of these granite suites.

The evolution trend of the Cretaceous tin granites of central Nigeria suggests a source material low in tin which appears to correspond to the important mantle component in these rocks (Sn content upper mantle: around 0.8 ppm; Anderson 1983). Efficient titanomagnetite fractionation is, however, feasible as an alternative explanation for the low tin content in early melt portions.

The Rb/Sr-Sn pattern of the central Thailand granites is similar to the Nigerian case (Fig. 84) and results from a mixed sample population which includes some of the chemically primitive Permian volcanic-arc granites of eastern Thailand, which are tin-barren. The extension of this volcanic-arc granite province into peninsular Malaysia (East Coast; "eastern granite belt") is host to some tin deposits in the most evolved granite intrusions. Geochemical and Sr and Nd isotope data indicate involvement of mantle material in this eastern granite belt in the SE Asian tin province (Liew and McCulloch 1985; Cobbing et al. 1986; Darbyshire pers. commun. 1988).

The correlation lines in Fig. 84 have a different slope m which, according to Eq. 12 in Chapter 2.2, is defined by $[\overline{D}_{Sn}-1]/[\overline{D}_{Rb/Sr}-1]$ and $[\overline{D}_{Sn}-1]/[\overline{D}_{TiO2}-1]$, respectively. The slope is therefore related to the magnitude of the bulk tin distribution coefficient $\overline{D}_{Sn}$. Flat correlation lines correspond to $\overline{D}_{Sn} \approx 1$, steep correlation lines point to $\overline{D}_{Sn} < 1$. There is a continuum in slopes for different granitic fractionation suites. The major tin granite suites in Fig. 84 all demonstrate a $\overline{D}_{Sn} < 1$, which explains their geochemical "specialization" in tin. On the other hand, non-tin granites display $\overline{D}_{Sn} \geq 1$. Our examples of non-tin granites are very limited because systematic analytical tin data for such rocks are scarce. The global average for granitic rocks of 3 ppm Sn (Turekian and Wedepohl 1961; Hamaguchi et al. 1964; Grohmann 1965) or 5.5 ppm Sn (Taylor and McLennan 1983) would suggest an average $\overline{D}_{Sn}$ near unity. However, the necessarily low degree of differentiation in large granite systems limits the validity of such an interpretation.

The bulk tin distribution coefficient is essentially controlled by modal composition of the solidifying material in equilibrium with the melt, and possibly also by oxygen fugacity of the system. Fe- and/or Ti-bearing mineral phases are the main tin carriers (Petrova and Legeydo 1965; Kovalenko et al. 1988). Therefore, with Fe-Ti minerals involved in decreasing proportions during progressive fractional crystallization of granitic melts, a dynamic character of $\overline{D}_{Sn}$ may be expected, i.e. a decrease of $\overline{D}_{Sn}$ with growing degree of fractionation. Such a trend was observed in some tin-bearing rocks by Antipin et al. (1981). However, the scatter in the tin data on our sample populations allows no such conclusion. The generally low content of opaque minerals (mainly Ti and Fe oxides and sulphides) in ilmenite-series granitic rocks as opposed to magnetite-series granitic rocks, is shown in Fig. 85, which exhibits a clear compositional distinction between tin-tungsten granites, molybdenum porphyries and copper porphyries.

The petrogenetic classification scheme of magnetite- versus ilmenite-dominated granite suites is geochemically based on different oxygen fugacity fO_2 in these two general melt/rock systems (Ishihara 1981). Some fO_2 data from tin granites and from other ore-bearing granitic environments are depicted in Fig. 86. The chemistry of biotites from the Erzgebirge granite suite allows definition of a trend of decreasing fO_2 towards the latest tin-mineralized granite phases, which spans about two log units from YG 1 to YG 3 and aplite (Förster and Tischendorf 1989). It is interesting to note that the Older Granites of the Erzgebirge (OG 1-3) reveal much higher $fO2$ conditions near the HM buffer (Förster and Tischendorf 1989, 1990). These granites are tin-barren but have locally associated molybdenum-tungsten mineralization. This situation is in accordance with the fO_2 data from the molybdenum
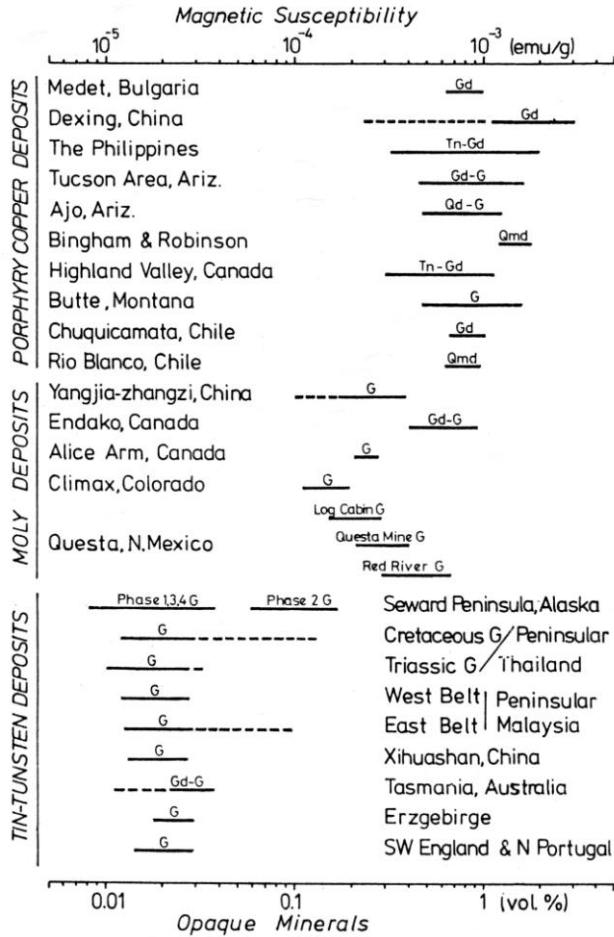
Fig. 85. Modal content of opaque minerals in granitic rocks related to Cu, Mo and Sn-W ore deposits (Ishihara 1981:474). **Tn** tonalite; **Qmd** quartz monzodiorite; **Gd** granodiorite; **G** granite. The limit between ilmenite- and magnetite-series granitic rocks is defined at 0.1 vol% of opaques (Ishihara 1977)

porphyry systems of Questa and Pine Grove, which have redox conditions above the NNO buffer. The fO_2 data from tin ore-related granite phases of the Erzgebirge, from Portugal, Cornwall and from the Seward Peninsula in Alaska plot in between the NNO and QFM buffer lines. The extension of this region towards lower temperature meets the fO_2 conditions typical for the early high-temperature stage in many tin deposits, defined by a position at or below the pyrite-magnetite-pyrrhotite buffer. Oxygen fugacity of tin granite systems at both the magmatic and hydrothermal stage is clearly different from copper porphyry systems (Fig. 86).
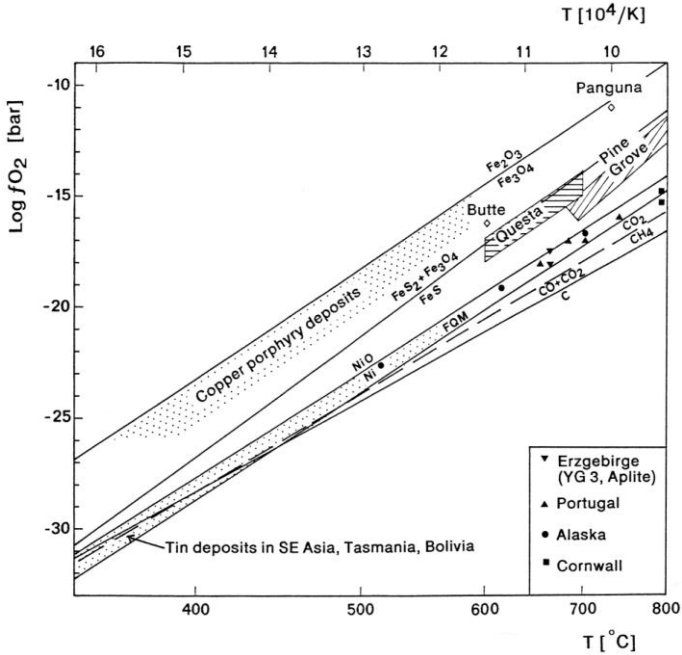
Fig. 86. Temperature and oxygen fugacity conditions of some magmatic-hydrothermal ore systems as defined by biotite or Fe-Ti-oxide composition and hydrothermal mineral or fluid inclusion equilibria. Data for Erzgebirge granites from Förster and Tischendorf (1989), Portuguese tin granites from Neiva (1976, 1982), Ear Mountain tin granites, Seward Peninsula, Alaska from Swanson et al. (1988), Cornubian granites from Charoy (1986) and Stone et al. (1988). Comparative data for molybdenum porphyries are from the Questa Caldera, New Mexico (Dillet and Czamanske 1987) and the Pine Grove system, Utah (Keith and Shanks 1988). Copper porphyry data are from Panguna-Bougainville, Papua New Guinea (Eastoe 1982) and Butte, Montana (pre-main stage mineralization; McKenzie and Helgeson 1985). The general compositional field for copper porphyry mineralization is defined by the equilibrium mineral assemblage magnetite-hematite (Burnham and Ohmoto 1980). The early hydrothermal conditions in tin ore formation are defined by a general position below the pyrite-pyrrhotite-magnetite buffer (cf. Kelly and Turneaure 1970) and by CO_2/CH_4 ratios in fluid inclusions (Renison Bell Mine, Tasmania: Patterson et al. 1981; SE-Asian tin belt: Jackson and Helgeson 1985b; Cornwall: Shepherd et al. 1985). CO_2-CH_4 equilibrium at 1 kbar is from Patterson et al. (1981); other sources for petrogenetic buffer lines are given in the legend of Fig. 9

Solubility data of tin in silicic melts strongly suggest that crystallization of magmatic cassiterite from a melt containing tin at the ppm level is unlikely (cf. Chap. 2.5). This is particularly unlikely in low fO_2-tin granites, even with tin contents of a highly fractionated melt at the 100 ppm level, but cassiterite saturation may occur in extremely fractionated pegmatite phases. The occasional mention of intramagmatic cassiterite and of intramagmatic tin ore deposits in the literature (Schröcke 1954, 1986) is based on equivocal petrographic evidence, i.e. the idiomorphic habit of cassiterite, which is, however, a general feature of this mineral at any stage of formation and is due to the interfacial energy of cassiterite.

6.4 The Transitional Magmatic-Hydrothermal System

The magmatic and hydrothermal systems in tin granite situations form a continuum characterized by complex transitional phenomena. The transitional stage begins with the differential release of a fluid phase at the solubility boundary of the melt-crystals system as a function of total pressure (level of intrusion), degree of solidification and initial fluid content in the melt. The transitional stage grades below the solidus into the hydrothermal stage. The mobility of the fluid phase depends on the nature and magnitude of permeability, which may lead both to fluid fixation/migration in the intergranular space and to fracture-focussed fluid convection. A consequence of fluid saturation may be fluidization of the residual magma, which may lead to the pervasive emplacement of such material into already crystallized and consolidated granite. Disruptive, secondary magmatic textures of a wide variety may result (see below). A dynamic system composed of multiple intrusions with episodic release of mechanical energy (internal hydraulic fracturing and/or external tectonics) may accumulate fluids in intergranular space which by fracturing may be intermittently tapped and collected on larger structures (reservoir model by Pollard and Taylor 1986). The comagmatic fluid exsolution and accumulation on intergranular space causes chemical and textural convergence between magmatic and hydrothermal mineral formation in granitic rocks, which is probably one of the reasons for the historical discussion of magmatism versus metasomatism in the origin of granites. The petrographical problem of magmatic versus sub-solidus muscovite arises from the same general situation.

The transitional stage in between a magmatic (xtls + melt) and a hydrothermal system (xtls + aqueous fluid), i.e. a system characterized by coexistence of

xtls + melt + aqueous fluid (aqueous fluid may under subcritical conditions separate into liquid and vapour phase) will have an abrupt character in the case of synchroneous fracturing and pressure release, and will be longer-lived under quiet pressure conditions. In the first case, favoured by a low-pressure regime at shallow levels, stockwork systems may develop, of which porphyry ore deposits are a fossil relic. The fracture-controlled open system of the porphyry-situation allows rapid and large-scale fluid circulation with concomitant chemical and pysical disequilibria between fluids and wall rocks. In the second case, the fluid phase remains trapped on interstitial spaces or on microcavities. Pegmatitic domains on a micro- to macro-scale may form in which the solidification of highly fractionated melt results in a volumetrically important fluid phase crystallizing in a closed system in equilibrium with the melt phase.

These two end-member scenarios arise as a consequence of the solubility of water in granitic melts (Niggli 1920). The importance of the violent release of a fluid phase in high-level environments was recently emphasized by Whitney (1975), Burnham (1979a,b, 1985) and Burnham and Ohmoto (1980). Supporting textural evidence for fluid exsolution can be found to some degree in any granitic intrusion. Magmatic-hydrothermal phenomena will, however, be most pronounced in strongly fractionated granites where the fluid-accommodating capacity of intergranular spaces may be exceeded. Field evidence for local fluid saturation in tin granites are aplite-pegmatite domains on a cm to m scale in the form of pods, lenses, pipes and veins with repetitive features of textural contrasts (fine-/coarse-grained) and mineral corrosion, and pockets on a microscopic to megascopic scale of quartz-feldspar mosaics. On the microscopic scale, there is a wide variety of textures produced by high-temperature fluid interaction (partially in equilibrium with the magmatic mineral assemblage) such as blebbing of feldspars by albite or secondary quartz, feldspar-quartz myrmekites, micrographic and symplectic intergrowths of quartz, feldspars and muscovite.

The microgranitic fabric of the most evolved tin granite phases is identical to experimental quenching fabrics produced by fluid release (Swanson 1977; Swanson et al. 1988). The fabric in many tin granite intrusions is characterized by two hiatal grain size populations consisting of medium- to coarse-grained quartz, feldspar and biotite porphyroclasts in a fine-grained quartz-feldspar-biotite matrix (microgranitic component). The proportion of megacrystic material to microgranitic groundmass is highly variable and is the reason for the variety of textures in some plutons. There is a continuous spectrum from primary textured "normal" granite to non-megacrystic microgranites, connected by "two-phase variants" (Cobbing et al. 1986). The field aspect of

these gradational two-phase variants is characterized in an incipient stage by the thin development of microgranite along grain boundaries in host granite (primary textured granite) and, with an increase in volume of the microgranitic component, leads to disruption of the host granite fabric and corrosion of its mineral constituents by the invading microgranitic matrix. These rocks are usually termed granite porphyries. The alternative term of "megacrystic microgranite" or "two-phase variant" emphasizes the two-phase crystallization process which is interpreted by Cobbing et al. (1986) and Cobbing et al. (in prep.) as a consequence of sudden loss of pressure in a shallow environment causing the residual melt to quench. This results in partial fluidization of the magma and its violent emplacement into, and disruption of the already consolidated primary textured host granite. Fluid penetration beyond the disruption front will produce non-disruptive recrystallization effects in the host granite accompanied by hydrothermal alteration.

The ratio of solid phases (crystals) to liquid (melt + aqueous fluid) will determine the degree of fluidization. According to Wohletz and Sheridan (1979:178), a fluidized system may be defined as "a mixture of particles (solid or liquid) suspended by an upward escaping fluid phase (liquid or gas) so that the frictional force between the fluid and the particles counterbalances the weight of the particles and the whole mass behaves as a fluid". Progressive stages in gas fluidization of solid particles generated by increasing flow rate of the gas phase may change from a fixed bed state, to a quiescent fluidized, to a turbulent fluidized state. The fixed bed state is characterized by an undisturbed grain pattern with fixed contacts between solid particles. Increasing fluid flow leads to a state where individual particles are free to

---

Fig. 87 (next page). Heterogeneous (secondary) magmatic textures from two-phase granites in the SE Asian tin belt, interpreted as disruptive emplacement of residual melt (fine grained matrix) into partially or wholly crystalline host granite (medium to coarse grained xenocrysts). Photographs from thin sections under oblique polars, length of plates is 20-30 mm. Photographs A and B by courtesy of John Cobbing, Nottingham.
A Xenocrysts of corroded quartzes and feldspars, sieved by quartz blebs, in microgranitic matrix. Dindings Pluton, near Kinta Valley, Malaysia. Sample no. 11 in Cobbing et al. (1986).
B Xenocrysts of corroded quartz, microcline, oligoclase and biotite in microgranitic matrix. Kuala Lumpur Pluton, Malaysia. Sample no. 232/94/416 in Cobbing (1989).
C Megacrystic microgranite composed of xenocrysts of microcline, oligoclase, quartz and brown biotite in fine-grained groundmass of same mineral composition. Tanjungpandan Pluton, Indonesia. Sample no. 217 in Lehmann (1988b)
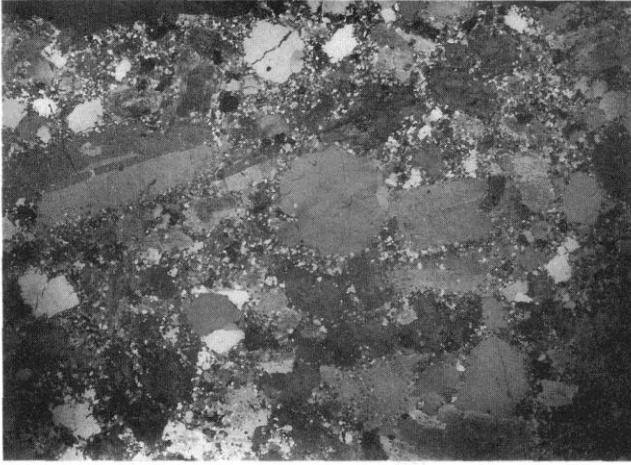
A
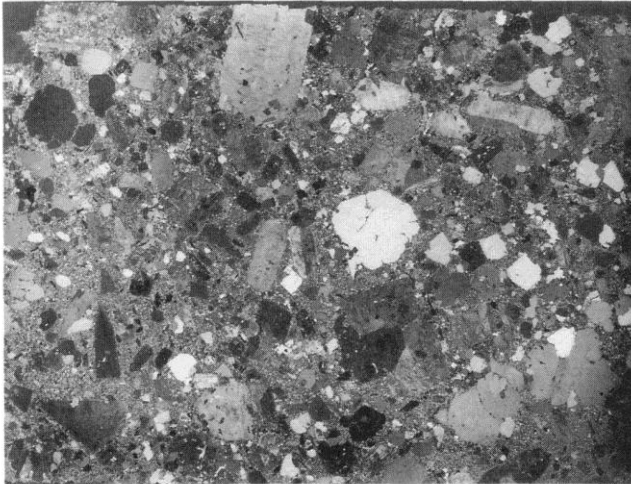
B

C

move and where textural integrity is lost. The "fluidizing point" (Leva 1959) is reached when the downward gravity force on the particles is balanced by the upward fluid drag. As fluid flow increases, simple grain separation by increasingly larger spacing is followed by progressively more violent agitation of particles in a turbulent state with abrasion and disaggregation of solid components and the formation of gas bubbles.

The above fluidization phenomena are well known from industrial processes. The most evident application to geological systems is explosive volcanism and breccia pipe formation (Reynolds 1954; Wohletz and Sheridan 1979; McCallum 1985), where turbulent fluidization is an essential feature. The textural patterns of granitic rocks, particularly of highly evolved and boron-rich low-solidus tin granites, suggest a variety of incipient stages of fluidization which are less spectacular and little studied but which contain probably essential physical information on the late magmatic-early hydrothermal evolution of granite plutons.

Secondary magmatic textures are a widespread feature in the granites of the SE Asian tin belt and are commonly associated with tin mineralization (Cobbing et al. 1986; Pitfield et al. 1990). Petrographically, they form a more or less continuous textural suite ranging from slightly disrupted primary texture granites through transitional types to essentially equigranular microgranites. This textural evolution corresponds to a sequence of geochemical evolution (Pitfield et al. 1990). Similar granite textures seem to be important in other tin granite provinces as well and are usually described as granite porphyries (Massif Central: Aubert 1969; Cornwall: Hall 1974; Bolivia: Lehmann 1979). Examples for secondary magmatic textures in tin-bearing granites in the SE Asian tin belt are given in Fig. 87.

Fluid release from within the magma as a result of second boiling provides an explanation for the fracture pattern in high-level granitic intrusions which is centred on late and most evolved intrusion phases; a situation typical of copper, as well as tin-tungsten and molybdenum porphyries/granites. The high salinity and stable isotope composition of early hydrothermal fluids in these deposits are in favour of a magmatic origin of the ore fluids which during the cooling history of the magmatic-hydrothermal systems become dominated by external fluids.

The transitional magmatic-hydrothermal stage (i.e. coexistence of crystals, melt and aqueous fluid) is the key condition for most models of pegmatite formation (Smith 1948; Jahns and Burnham 1969; Cerny 1982). Extreme variations in grain size in miarolitic rare-metal bearing pegmatites, particularly
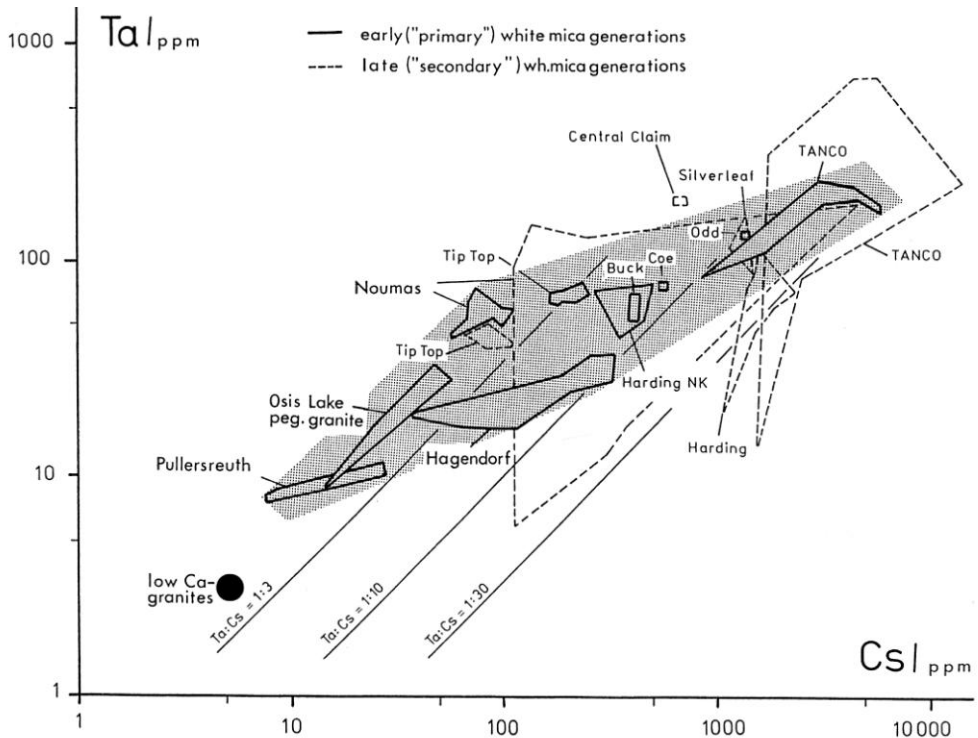
Fig. 88. Ta-Cs variation diagram for white micas from various granitic pegmatites (Gaupp et al. 1984; redrawn in Möller 1989:110). Shaded compositional field delineates data on early (primary) micas. Solid circle locates whole-rock composition of low-Ca granites. Strong Ta mineralization is associated with the Tanco, Silverleaf, Odd West, Buck Claim, Coe Claim, Central Claim pegmatites (Winnipeg River pegmatite district, Manitoba, Canada); moderate Ta mineralization is associated with the Harding pegmatite (New Mexico, USA), Tip Top pegmatite (Black Hills, South Dakota, USA), and Noumas pegmatite (Namaqualand, RSA); the ceramic pegmatites of Hagendorf and Pullersreuth (Oberpfalz, Bavaria, Germany) have no metal mineralization.

the typical association of aplitic and very-coarse grained domains, point to crystallization from two physically different fluids in the sense of the classical model by Jahns and Burnham (1969). The clear distinction between a granitic silicate liquid (melt) and a coexisting, comparatively low-density, saline aqueous fluid must, however, not be the case in boron-rich granite pegmatite systems, in which the pegmatitic fluid appears to have evolved continuously from a magmatic towards a hydrothermal state (London 1986).

A high degree of fractionation in Sn- and Ta-bearing pegmatites is indicated by the same systematic enrichment and depletion patterns which are typical

of tin granites. Compositional fields of white micas from a variety of pegmatites are given in Fig. 88 in terms of Ta versus Cs. Corresponding whole-rock data from alkalifeldspar aplogranite stocks of the Erzgebirge (Tischendorf 1989) would plot in an intermediate position in the compositional field for pegmatitic micas in Fig. 88.

Ratios of chemically coherent elements such as K/Rb, Ga/Al, Ta/Nb and Zr/Hf reach anomalous values in rare-metal pegmatites and follow the same trend line as highly fractionated granites (Cerny, 1982, 1989; Möller 1989). Cassiterite and zircon samples from pegmatites are characterized by Zr/Hf ratios of 4 ±2, those from hydrothermal vein deposits have ratios of 28 ±10, whereas average zircons and rocks of terrestrial and meteoritic origin have a Zr/Hf ratio of 43 ±8 (Möller and Dulski 1983; Cerny et al. 1985). The extremely low Zr/Hf ratio in cassiterite of pegmatitic origin points to a degree of fractionation F of less than 10^{-4} (Möller and Dulski 1983).

The extremely fractionated nature of Sn-Ta enriched pegmatite melts/fluids (enriched in other incompatible components such as H_2O, F, B, Li, Rb, Cs, Be) results in low viscosity and density of such systems which, given suitable
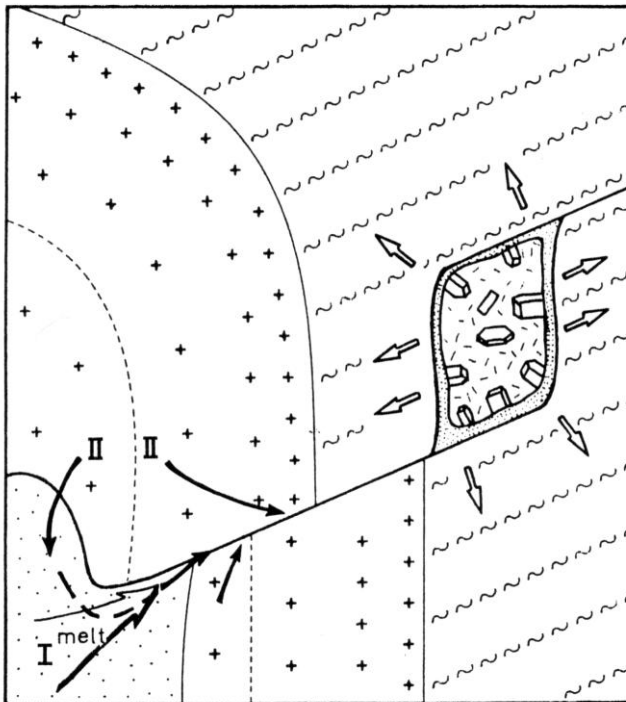
Fig. 89. Schematic two-component model of granitic pegmatite formation (Möller 1989:120). Fluid I is a late residual hydrous granitic melt, fluid II represents the intergranular liquid from crystallized granite which mixes continuously with fluid I

channelways, may migrate upwards and outwards of their granitic parent intrusion along fractures or zones of weakness. The most fractionated melt batches are the most mobile, which is seen as the reason for the zonal distribution of pegmatite types and associated metal mineralization in the roof of granite intrusions (Cerny 1989). The contact between different granite units or granite and country rock can be a favorable zone for pegmatitic fluid migration towards the most apical parts of granite intrusions. In the Erzgebirge, pegmatite zones along such contacts are known under the traditional term of "stockscheider", which consists mainly of coarse-grained K-feldspar, quartz, Li-bearing mica, and - locally - columnar aggregations of topaz (pycnite).

Alteration haloes around pegmatite bodies, heterogeneous $^{18}O/^{16}O$, D/H, $^{87}Sr/^{86}Sr$ and disturbed Rb-Sr patterns, and fluid inclusion evidence (Roedder 1984) point to a partly open system during pegmatite crystallization. The model of pegmatite formation by Möller (1989) envisions a combination of both a process of internal magmatic evolution (granitic and pegmatitic fluids) through fractional crystallization and a second process of mixing with intergranular fluids from the crystallized granite parent (Fig. 89).

6.5 The Hydrothermal System

The mobility of tin in hydrothermal solutions is, of course, independent of the origin of the aqueous phase and is essentially controlled by temperature, salinity and oxygen fugacity (Wilson and Eugster 1984; Eugster and Wilson 1985; Jackson and Helgeson 1985a; Haselton and d'Angelo 1986; Kovalenko et al. 1986). The optimal constellation of these parameters is given at high salinity and temperature and low fO_2. An aqueous phase in a tin granite system (at or below NNO buffer) at subsolidus temperatures of 500-600 °C will have a tin-transporting capacity of several hundred to several thousand ppm Sn (cf. Chapts. 2.6 and 2.7). Whether such high tin concentrations can be reached at any point, depends on the primary tin content and the fixation of tin in the percolated rocks, from which tin may be released by a variety of congruent or incongruent dissolution and exchange reactions. It can be expected that part of the residual aqueous fluids of magmatic origin is trapped on grain boundaries or microcavities in the rock, thus providing a vast fluid reservoir (Pollard and Taylor (1986). These interstitial fluids can migrate to higher structural levels under the influence of thermal and pressure gradients, or can be flushed out by external fluids such as ingressing meteoric water.

Leaching of biotite together with muscovitization and chloritization may be another mechanism of tin release, suggested early on by Barsukov (1957).

Repeated dissolution of hydrothermal cassiterite and crystallization of high-grade tin ore is favoured by a fluid system which is not entirely buffered by its granitic wall rocks (equilibrium assemblage quartz-feldspar-muscovite) and where a decreasing pH during fluid cooling allows high tin contents in the hydrothermal fluid down to temperatures of 200-250°C (Heinrich and Jaireth 1989). Low-pH conditions of a fluid-buffered hydrothermal evolution are possible in spatially restricted circulation systems such as quartz veins or greisen environments in which feldspar was previously destroyed.

Efficient hydrothermal leaching, transport and deposition of tin apparently need a magmatically tin-preenriched reservoir on which the hydrothermal extraction process must be focussed. This is in contrast to the metallogeny of gold and base metals, for instance, and must be the reason why economic tin concentrations in high-temperature, low-pH and low-fO_2 hydrothermal systems not related to a tin-enriched rock volume are so rare. Favourable conditions for tin leaching and transport can, for example, be expected in such parts of hydrothermal systems at mid-ocean ridges where the fluid is rock-buffered by mantle material at a redox state up to four log units below FMQ, i.e. at the iron-wüstite buffer (Bryndzia et al. 1989). Although cassiterite occurrences from such a setting have been reported, these are very small tin concentrations only, compared to the much more efficient extraction and enrichment processes for base metals (Dmitriev et al. 1971; Jankovic 1972). The locally high tin content in volcanogenic massive sulphide deposits, which permits in some cases a by-production of tin, is probably understandable as the result of such a low-fO_2 environment. A countercurrent distribution pattern of tin and gold can be predicted as a consequence of the complementary solubility behaviour of the two redox couples Au^+-Au^0 and Sn^{2+}-Sn^{4+}, i.e. tin fixation (cassiterite precipitation) under relatively more oxidized conditions and gold precipitation in more reduced parts of the same hydrothermal system (given a sulfidation state inside H_2S stability field).

The fact that tin deposits have such a strong preference for highly fractionated granitic rocks, in which tin is enriched about one order of magnitude over average crust, is not fully explainable by the tin specialization alone of their host environments. Otherwise, small-scale tin deposits should be much more abundant in non-granitic terranes. Highly fractionated granitic systems apparently not only provide the chemical inventory for tin ore formation, but also provide this inventory in a framework which allows efficient extraction

and hydrothermal redistribution. This situation is probably a consequence of the interstitial fluid release during granitic crystallization.

The formation temperature of cassiterite in tin ore deposits is commonly in the range of 300-500°C as noted in the first summary study by Little (1960) and later confirmed by numerous investigations. Occurrences of colloidal wood tin (hydro-cassiterite) in Mexico seem to have formed at a temperature as low as about 150°C (Pan 1974). Salinity data from fluid inclusions in cassiterite and associated quartz vary widely between 1 and >50 wt% NaCl-equivalent, with a typical average range of 5-20 wt% (1-4 m NaCl) (Bolivia: Kelly and Turneaure 1970; Grant et al. 1977; Erzgebirge: Durisova et al. 1979; Thomas 1982; Tasmania: Patterson et al. 1981; Portugal: Kelly and Rye 1979; Cornwall: Jackson et al. 1982; Nigeria: Kinnaird 1985; and general review in Roedder 1984). The hydrothermal conditions during cassiterite crystallization, as derived from the study of fluid inclusions, correspond to the solubility range of a few to a few hundred ppm Sn.

It should be borne in mind that fluid inclusion data record the depositional regime of the minerals investigated, i.e. the final stage in the evolution of an ore fluid. The stable isotope data from tin ore deposits uniformly indicate that the tin-mineralizing fluids were equilibrated isotopically (and probably chemically) with a hot (T > 400-500°C) granitic mineral assemblage, prior to their transport into a cooler ore deposition site (Kelly and Rye 1979; Grant et al. 1980; Patterson et al. 1981; Pollard and Taylor 1986; Sun and Eadington 1987; Thorn 1988).

Oxygen fugacity during tin ore formation can be reconstructed from the mineral paragenesis and composition of fluid inclusions. A worldwide feature of tin deposits is an early high-temperature stage of pyrrhotite ± pyrite followed by a late stage (post-cassiterite mineralization) of pyrrhotite alteration in which pyrrhotite is pseudomorphically transformed into pyrite/marcasite ± siderite (see Kelly and Turneaure 1970). Pyrite blastesis tends to completely extinguish the primary pyrrhotite fabric. The occurrence of magnetite (often as inclusions in cassiterite and in fluid inclusions) together with pyrrhotite ± pyrite defines an upper fO_2 limit at the pyrrhotite-pyrite-magnetite buffer. The lower fO_2 limit is given by the ratio CO_2/CH_4 in fluid inclusions. This ratio is >1 for most tin deposits (temperature: 350-400°C). In many cases CH_4 is not detectible, in some deposits CO_2/CH_4 is around unity (Tikus, Indonesia: Schwartz and Surjono 1988; Renison Bell, Australia: Patterson et al. 1981; Sa Moeng, Thailand: Khositanont in prep.). These observations suggest an fO_2 interval for cassiterite formation in between the pyrrhotite-pyrite-magnetite (at 350°C nearly identical to NNO) and the QFM
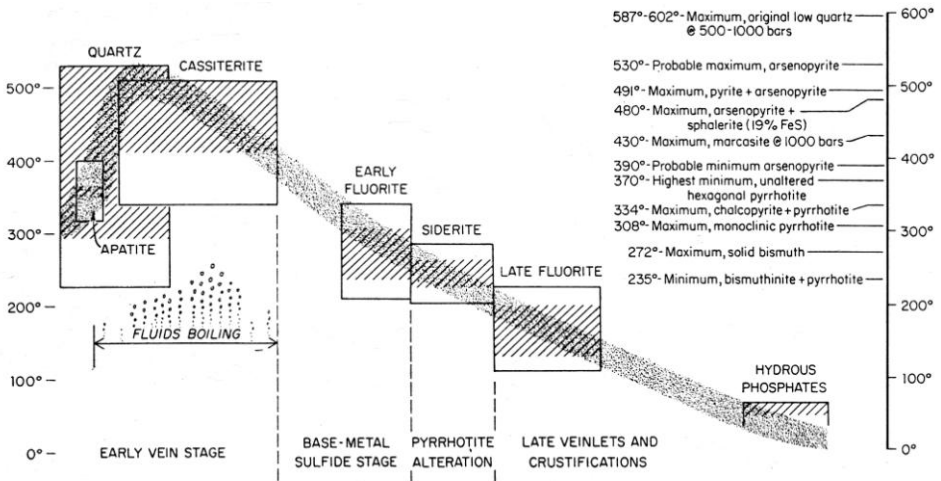
Fig. 90. Generalized temperature evolution of tin-tungsten deposits in the Bolivian tin belt, derived from fluid inclusion data and from mineral equilibria (Kelly and Turneaure 1970:673). Typical mineral assemblages are (Kelly and Tuneaure 1970; Hanus 1982; Wolf and Sanchez 1976). **1** Early vein stage: quartz-muscovite-tourmaline-apatite-cassiterite-wolframite-löllingite/arsenopyrite-fluorite-siderite-chlorite. **2** Base-metal sulphide stage: pyrrhotite-arsenopyrite-sphalerite-bismuth-bismuthinite-chalcopyrite-stannite-galena. **3** Epithermal stage: pyrite-marcasite-siderite (reaction paragenesis from pyrrhotite alteration); complex sulphides-stibnite, Bi-Co-Ni-Ag-U sequence and gold, fluorite-baryte-phosphates-limonite-gold-silver (low-temperature remobilization)

reference buffers. This is the same interval which, at higher temperature, characterizes the crystallization of tin granites (Fig. 86), and is probably a consequence of the broad-scale control of the hydrothermal system by its granitic wall rocks, at least in an early stage with a low water/rock ratio. A trend of increasingly external influence on the hydrothermal system can move the fluids and their wall rocks at a later stage into the hematite stability field.

Figure 90 summarizes the typical temperature evolution and mineralogical sequence in hydrothermal tin deposits. The diagram is from the classical work by Kelly and Turneaure (1970) who studied over fifty tin and tungsten deposits in Bolivia which in spite of different ages and genetic types gave a uniform evolutionary pattern. This pattern, although in individual deposits commonly not developed in full, provides a general framework with respect to temperature and mineral association in tin ore formation.

Fluid oversaturation and precipitation of cassiterite in those paleo-solution channels which are today's tin deposits is a consequence of one or several processes which, according to Figs. 13 and 14, lead to cassiterite formation: decrease in temperature and/or chloride activity, increase in fO_2 and/or pH. All these processes can be caused and influenced by mixing with meteoric water and interaction with wall rocks. A predominantly meteoric water component is typical for the later stages of hydrothermal evolution in tin ore systems, as seen in D/H isotope patterns in many localities (Cornwall: Jackson et al. 1982; Portugal: Kelly and Rye 1979; Thailand: Lehmann 1988a; Bolivia: Grant et al. 1980; etc.).

Cassiterite precipitation according to the general equilibrium

$$Sn^{2+} + H_2O + \tfrac{1}{2}O_2 = SnO_2 + 2H^+ \tag{26}$$

is redox- and pH-dependent and must therefore be accompanied by H^+- and H_2-consuming processes. Acid neutralization is most effectively achieved in carbonate rocks during the formation of skarn or sulphide replacement tin deposits by the model reaction

$$Sn^{2+} + CaCO_3 + H_2O = SnO_2 + Ca^{2+} + CO_2 + H_2 \qquad . \tag{27}$$
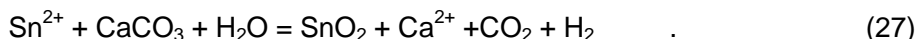
Feldspar-destructive wall rock alteration seems to be the dominant H^+-consuming reaction in non-carbonate rocks in which muscovitization is an important feature, such as:

$$Sn^{2+} + 3(Na,K)AlSi_3O_8 + 2H_2O =$$
$$SnO_2 + KAl_3Si_3O_{10}(OH)_2 + 6SiO_2 + 2Na + H_2. \tag{28}$$

The commonly observed paragenetic mineral assemblage cassiterite + arsenopyrite has been proposed by Heinrich and Eadington (1986) as a wall rock-independent redox buffer. Precipitation of arsenopyrite by reduction of As^{3+} complexes may couple with oxidation of Sn^{2+} complexes to precipitate cassiterite:

$$3Sn^{2+} + 2H_3AsO_3 + 2Fe^{2+} + 2H_2S = 3SnO_2 + 2FeAsS + 10H^+ \tag{29}$$
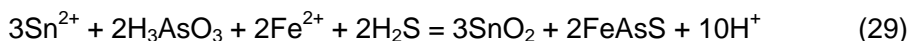
An alternative redox couple for fluid-buffered cassiterite precipitation in CO_2 rich fluids is possible through the equilibrium $CO_2 + 4H_2 = CH_4 + 2H_2O$ (Giggenbach 1980).

6.6 Synthesis

Tin ore deposits are part of fossil hydrothermal systems centred on highly fractionated late phases of extended granitic fractionation suites. These hydrothermal systems are developed in apical high-level portions of granitic intrusion series, and their association with granitic magmatism typically developed in active uplift regions (Pitcher 1979, 1987), makes them extremely sensitive to erosional processes. Primary tin ore deposits, in association with granitic rocks of collisional belts and in back-arc regions, are therefore mostly Mesozoic-Cenozoic in age, whereas tin granite systems in anorogenic intracratonic settings can be traced back to Archaean times. A similar situation can be found for copper and molybdenum ore deposits in association with granitic magmatism.

The granitic phases/subintrusions in spatial, temporal, and chemical relationship to tin ore deposits (i.e. tin granites) are highly fractionated. According to systematic trace element distribution patterns in these subunits and in associated larger granite systems, fractional crystallization seems to be the dominant petrogenetic process controlling magmatic evolution. Convective fractionation, i.e. convection of fluid away from crystals, provides an effective crystal-melt separation mechanism (Rice 1981; Sparks et al. 1984). The multiphase nature of the intrusion systems and their systematic enrichment patterns in incompatible trace elements towards the youngest and volumetrically smallest phases point to a crystallization process from the plutonic margins inwards (Groves and McCarthy 1978) and episodic tapping of an increasingly fractionated and buoyant magma chamber below the gradually deepening solidification front.

Sr and Nd isotope data indicate for most tin granite suites an origin predominantly by partial melting of crustal material; in some tin provinces a substantial mantle component seems to be involved. The starting material of the granitic fractionation suites has no anomalous contents in tin as compared to average pelitic material. The tin specialization of tin granites is a consequence of their magmatic evolution by fractional crystallization, and crustal thickness may be an important parameter in influencing the magma residence time and its spatial evolution. This is suggested by the more continental setting of tin granite systems as compared to the chemically less evolved copper porphyries. The origin from mantle or crustal sources is probably secondary to the importance of fractionation mechanisms because the ratio of tin content of bulk crust to upper mantle is only two to four.

Oxidation state (conventionally described by oxygen fugacity fO_2) seems to control the bulk tin distribution coefficient $\overline{D}_{Sn}$(crystals/melt), i.e. degree of magmatic tin enrichment during fractional crystallization, in influencing the Sn^{4+}/Sn^{2+} ratio in the melt. Contrary to the behaviour of molybdenum which is enriched in molybdenum porphyries at $fO_2 >$ NNO (Ni-NiO buffer), tin granites are characterized by conditions of $fO_2 <$ NNO. This difference is reflected by the magnetite-series mineralogy in granitic systems associated with molybdenum ore deposits, whereas tin-bearing systems are associated with ilmenite-series granitic rocks (Ishihara 1981). Other factors influence $\overline{D}_{Sn}$ as well, which are again dependent on degree of fractionation. As crystallization proceeds, $\overline{D}_{Sn}$ can be expected to decrease towards late crystallization stages, due to a modal increase in mineral phases with low partition coefficients $\overline{D}_{Sn}$. The increasingly depolymerized melt structure during fractional crystallization as a result of the enrichment in H_2O, B, F may, in addition, further decrease $\overline{D}_{Sn}$ by reducing individual mineral partition coefficients $\overline{D}_{Sn}$ (Antipin et al. 1981).

Degree of fractionation and oxidation state are the two parameters of prime importance for magmatic tin enrichment in granite suites, and have a regional control over the formation of tin provinces. Degree of partial melting seems to be of lesser importance in granite systems because the physical process of silicic melt separation during anatexis probably limits the relevant range of degree of partial melting to 20-50 % (Compston and Chappell 1979; Thompson and Connolly 1990). Low oxygen fugacity in granitic melt could be provided by source material with high Fe^{2+}/Fe^{3+} ratio and/or high carbon or S^{2-} content. Pelitic sedimentary sequences on the order of 10 km of stratigraphic thickness are typical for the basement of many tin provinces (SE Asia, Bolivia, Cornwall, Portugal). Pelitic source rock material makes little difference to the magmatic tin distribution patterns in tin granites as compared to other source rocks. However, the extreme boron enrichment of most tin granite systems may reflect the distinct boron enrichment of average shale (100-200 ppm B) as compared to bulk crust (10 ppm B), whereas the corresponding tin data are 2.5 ppm (bulk crust) and 3-5 ppm (shale) (Taylor and McLennan 1985). An indication for pelitic source rock material in most (but not all) tin granite suites is the generally peraluminous S-type character of these granites, which contrasts with I-type fractionation suites associated with F-dominated molybdenum ore systems.

The hydrothermal tin ore system is a continuation and result of the magmatic evolution trend, with shallow intrusion level providing high permeability and fluid circulation. The exsolution of a chloride-bearing fluid phase from a crystallizing granitic melt is the necessary consequence of anhydrous

crystallization of a hydrous melt (Holland 1972). The exsolved fluid phase can be accommodated and stored by the intergranular space in little fractionated magma portions. In higher fractionated melt portions, larger physical domains of a fluid phase will form during solidification, accompanied by focussed development of mechanical energy during retrograde boiling (Burnham 1985). The symmetry of structurally controlled permeability patterns centred on apical portions of highly evolved granite stocks argues for such a situation which is particularly developed in subvolcanic settings (porphyry-type stockworks, pervasive brecciation, breccia pipes).

A continuum may be expected in between the more static fluid storage in intergranular spaces and explosive fluid-melt phenomena. A two-phase crystallization pattern is typical of highly fractionated granites, with a primary medium- or coarse-grained granitic fabric forcefully invaded and partly corroded by fine-grained material of similar composition. The ratio between both phases is highly variable on a metre- to centimetre-scale. The bimodal grain distribution and locally pervasive disruption of the primary fabric by very mobile late-magmatic, fine-grained material with development of blastomylonitic textures suggests coexistence of crystals and melt with a fluid phase under $p_{fluid} > p_{lithostatic}$. The identity of the resulting rock as a porphyroclastic or megacrystic microgranite and its wide distribution in granite provinces has only recently been demonstrated by regional granite mapping programmes in SE Asia (Cobbing et al. 1986). Two-phase rocks under the conventional description as granite porphyry or porphyritic granite are generally well known to be associated with tin mineralization.

The mobilization of the magmatically developed tin potential in a highly fractionated granite phase is possible both in the earliest stage of magmatic fluid release as well as during later invasion of the cooling intrusive system by meteoric water. Initially, there will be a separation of both fluid systems, due to the extremely low permeability of a melt. Fracturing during the sub-solidus evolution will lead to superposition and mixing of both fluid systems. The time span of tin mineralization in some ore deposits is on the order of several million years, which points to the existence of long-lived hydrothermal fluid circulation at high temperatures (>300°C).

The hydrothermal mobility of tin is physically controlled by the nature and extent of permeability and available fluid volumina during the subsolidus cooling history of a tin granite. Both factors are favoured in high-level environments. The chemical parameters pH, fO_2 and chloride activity control the tin carrying capability of a solution. Fluid-buffered low-pH conditions in hydrothermally altered rock portions (feldspar unstable) can sustain high tin

contents in hydrothermal solutions even at 200°C (Heinrich and Jaireth 1989).

Size and primary tin content of a granite system define the maximum quantity of extractable metal. The greatest hydrothermal tin enrichments in individual ore systems are on the order of 10^6 t Sn (ore deposit plus primary dispersion halo; e.g. Llallagua, Bolivia, or Altenberg, Germany). Tin granite subintrusions reach average primary tin levels of around 30 ppm. The hydrothermal depletion of a tin-enriched magmatic system must therefore comprise a large rock volume of up to 40 km^3, when an extraction rate of one third (10 ppm Sn) is assumed. The whole magmatic fractionation system must be at least ten times larger in order to produce a highly fractionated tin granite subintrusion.

The limiting assumption of Rayleigh fractionation with $\overline{D}_{Sn}=0$ gives a minimum size of the total magmatic system of 400 km^3. More realistic conditions of a less perfect fractionation mechanism require a total melt volume on the order of 1000-2000 km^3. This is the size of magma chambers known to be associated with some caldera eruptions (Hildreth 1981). The granite batholiths underlying the Erzgebirge and Cornwall tin provinces are about 50 times larger (Tischendorf 1989; Willis-Richards and Jackson 1989).

The process of hydrothermal tin extraction results in open-system distortions of primary magmatic tin distribution patterns (scatter distributions with tin deficiencies). Often however, hydrothermal tin depletion cannot be identified clearly, which suggests relatively small extraction rates not distinguishable from the internal scatter in (pseudo)-magmatic tin enrichment trends.

A synoptic view of the magmatic and hydrothermal evolution of a tin-bearing granite system is given in Fig. 91 in conceptual analogy to copper porphyry systems (Burnham 1979a):

1. Intrusion of a granite body: sidewall crystallization combined with a onvective crystal-melt separation mechanism results in progressive fractionation of residual liquid. Thermal anomaly induces external meteoric-hydrothermal convection system. Solidifying magma portions release fluid into intergranular space.

2. Subintrusions of higher fractionated and less dense magma blobs develop in response to buoyancy and, possibly, tectonic squeezing. Solidus temperature decreases with increasing degree of fractionation, i.e. with enrichment in H_2O, F, B. Retrograde boiling during crystallization leads to magmatic fluid release with concomitant release of mechanical energy (stockwork and breccia formation); convergence between magmatic-
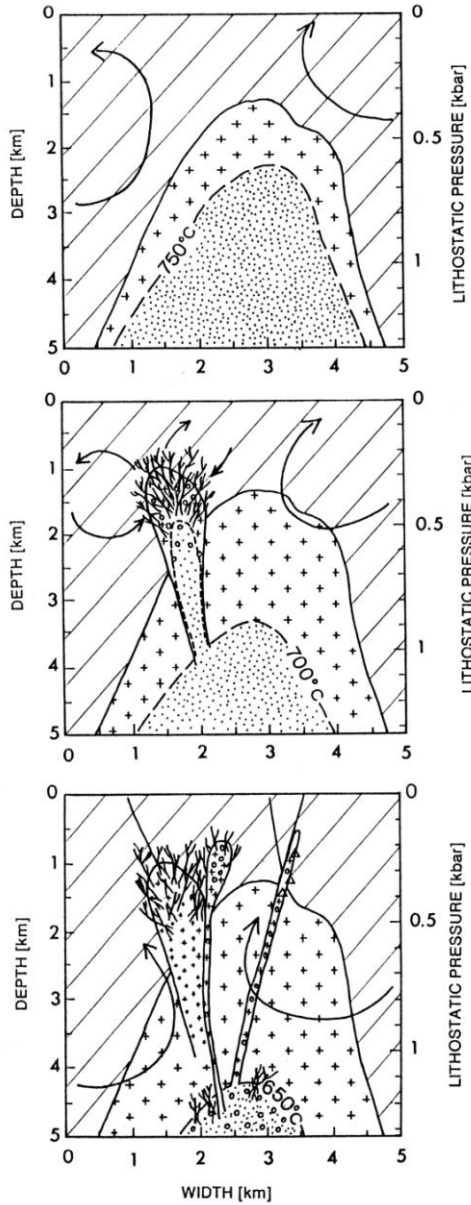
Fig. 91. Three stages in the schematic evolution of a tin granite system (5 x 5 km sections) in the upper part of a larger granite batholith. Arrows indicate trends of large-scale fluid movement. Broken-line contour in granite pluton marks solidus zone. Circle pattern represents zone of vapour release. For further explanation see text
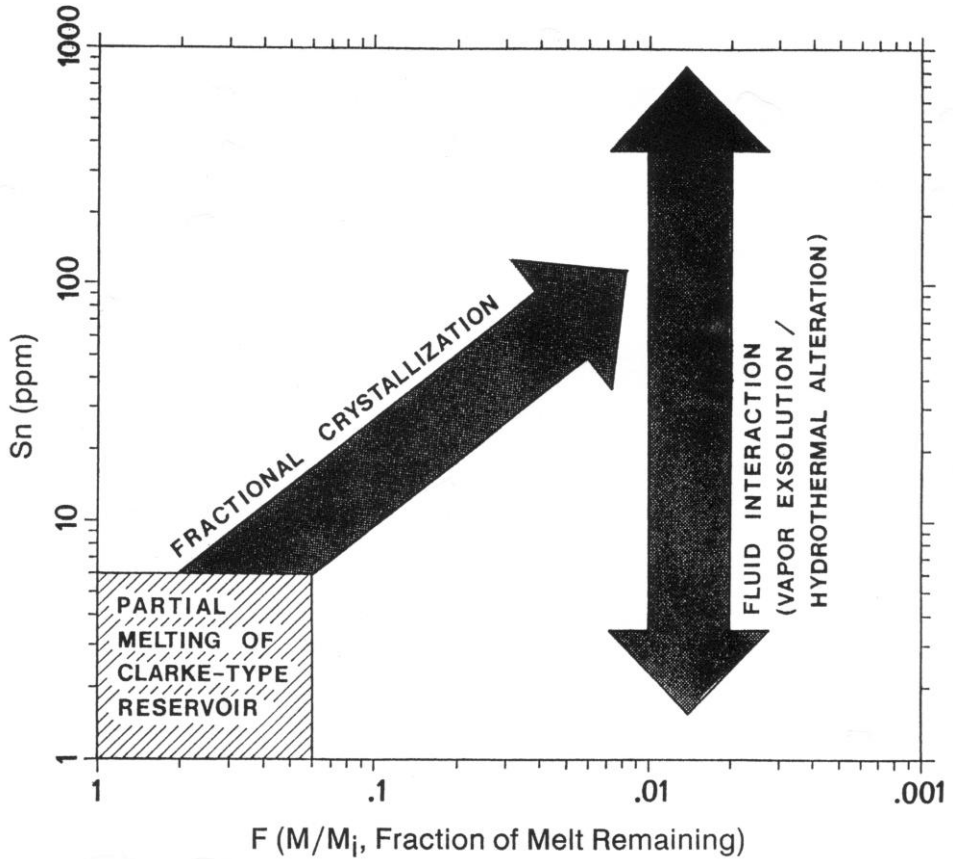
Fig. 92. Metallogenic model of tin ore formation: magmatic tin enrichment through fractional crystallization with $\overline{D}_{Sn}$(xtls/melt) <1, and subsequent hydrothermal redistribution of tin. Both processes are favoured by an oxidation state of the system below the NNO buffer

hydrothermal and meteoric-hydrothermal fluid systems with temporally increasing dominance of the meteoric fluid component.

3. Retreating solidification front in the plutonic main system with tendency towards fluid saturation during crystallization of residual melt; subintrusion of microgranitic stocks and aplite/pegmatite dykes with individual fluid and energy release: hydrothermal breccias and fluidization phenomena in the crystal-melt-vapour system. Fluid release at deeper levels and thermal contraction produce deeply penetrating tectonic structures. Increasing ingress of meteoric fluids and flushing out of interstitially stored residual magmatic fluids during decreasing temperature results in greisenization, potassic, sericitic, argillic, propylitic alteration etc. (systematic alteration patterns in analogy to other granite-related hydrothermal systems).

Focussing of the hydrothermal system according to local permeability conditions and cassiterite deposition as consequence of local physical and chemical gradients leads to the variety of the tin ore deposit spectrum (pegmatite, greisen, stockwork/vein, skarn/sulphide replacement).

The same general model is condensed in Fig. 92 under a geochemical point of view. The metallogenic model has two basic features (Lehmann and Mahawat 1989):

1. Magmatic tin enrichment trend: fractional crystallization of granitic melt with a bulk tin distribution coefficient $\overline{D}_{Sn}$(xtls/melt) <1. This condition is realized in peraluminous, ilmenite-series granitic rocks with an oxygen fugacity below NNO, which in turn is a precondition for effective hydrothermal depletion of magmatically tin-enriched rock volumes.

2. Hydrothermal tin redistribution pattern: magmatic fluid release during solidification of the highly fractionated tin granite system combined with interaction of the solidified granite with meteoric-hydrothermal fluids. Loading of the hydrothermal system with magmatically enriched tin, and cassiterite deposition according to local physicochemical gradients.